Geometrical Parameters of Rectangular AFM Cantilevers Producing Highest Sensitivity in Excitation of Second Mode in Air Environment

M. Damircheli*
Department of Mechanical Engineering,
Islamic Azad University, Shahr-e-Qods Branch, Tehran, Iran
E-mail: m.damircheli@qodsiau.ac.ir
*Corresponding author

Received: 6 March 2017, Revised: 23 April 2017, Accepted: 8 May 2017

Abstract: Today, improving the quality of the images acquired by the atomic force microscope (AFM) and obtaining the close properties of various samples are among the most important and challenging issues tackled by researchers. One of the key mechanisms of achieving these objectives is the excitation of higher modes, which raises the sensitivity of the AFM and consequently improves the resolution. To attain this goal, it is imperative to design or select a type of cantilever which is able to excite the second mode and produce maximum sensitivity in higher modes, especially the second mode. In this paper, an AFM cantilever with rectangular cross section has been investigated in air medium. The cantilever has been modeled by the Timoshenko beam model and the normal and tangential forces between cantilever tip and sample have been considered in the simulations. By changing the geometrical parameters of the AFM's cantilever and tip including length, width, thickness of cantilever, the angle between cantilever and sample surface, mass of tip, length of tip and Radius of tip, the frequency ratio of the second mode to first mode varies. The geometrical parameters that produce the minimum frequency ratio can increase the self-excitation probability of the second mode due to the excitation of the first mode simultaneously. The optimum geometrical parameters are derived that can increase the chance of higher mode excitation. The results indicate that the sensitivity of the second mode to sample stiffness also increases optimal geometrical parameters that yield the minimum frequency ratio; and, as a result, a higher contrast is achieved and it leads users to utilize the cantilevers with optimum geometry for achieving best contrast in imaging and properties estimation of unknown samples.

Keywords: AFM, Geometry, Higher modes self-excitation

Reference: Damircheli, M., "Geometrical Parameters of Rectangular AFM Cantilevers Producing the Highest Sensitivity in the Excitation of Second Mode in Air Environment ", Int J of Advanced Design and Manufacturing Technology, Vol. 10/ No. 3, 2017, pp. 51–58.

Biographical notes: M. Damircheli is PhD student of Mechanical Engineering at the Science and Research Branch, Islamic Azad University, Tehran, Iran. His current research focus is nanocomposites.

1 INTRODUCTION

The atomic force microscope plays an important and undeniable role in measuring properties such as surface topography, friction, viscoelasticity, elasticity modulus and shear modulus of samples. Many of the measurements acquired by the AFMs are based on the static bending of cantilever; however, the dynamic mode of AFM (i.e., dAFM) is much more sensitive and accurate; and in many applications, it is preferred over the static mode [1]. recently, the dAFM is extensively used for obtaining images from biological samples at nano scale. In the dynamic mode, the cantilever is made to vibrate at a frequency near its main frequency or frequencies, and the changes of frequency in the frequency modulation (FM-AFM) or the changes of amplitude in the amplitude modulation (AM-AFM) are used to get the topography or to obtain the properties of the investigated sample [2-5]. Nowadays bimodal and multi-frequency AFM (excitation of two or several modes together) can enhance spatial resolution of image, compositional contrasts and quantitative mapping of material properties.

In intermittent contacts between cantilever tip and sample, the existing nonlinear forces between them cause the cantilever to vibrate at higher modes and harmonics [6], [7]. Recently, numerous research works have been conducted on the advantages of exciting the higher harmonics and modes in the dynamic atomic force microscope. Stark et al. have investigated the rise in the sensitivity of the AFM due to the excitation of higher harmonics [8]. Sharos et al. have demonstrated that, by exciting the higher modes, the crime detection sensitivity goes up considerably [9]. other researchers have discovered that, in certain cantilevers or operating mediums (e.g., liquid medium), the second mode is automatically and spontaneously excited due to the excitation of the first mode at a time close the time of contact between tip and cantilever; and therefore, the dynamics of these systems is a multimode dynamics [10], and this spontaneous second mode excitation occurs because of the transfer of energy to the second mode from the force of interaction between tip and sample [11].

A multi-frequency atomic force microscope is a type of system in which several modes are excited simultaneously [12]. This idea was initially presented by Garcia et al. In this system, the output channels are much more than those of the single-mode excitation; and, therefore, with more outputs, we will be able to improve the resolution of the images and get a better approximation of sample properties [13]. considering the cited advantages for multi-frequency microscopes, designing a cantilever with the ability of self-exciting the second mode will greatly help us in acquiring higher resolution images and getting a more accurate approximation of sample properties. Obviously, the closer the frequency of the second mode is to that of the first mode, the higher the probability of the second mode excitation will be. Sadewasser et al. considered the length and width of a cantilever that could yield the minimum second-to-first mode frequency ratio as the optimal dimensions, and compare the images obtained by exciting the second mode of the cantilever with optimal dimensions with the images acquired by the first mode. Their results clearly showed the higher accuracy and resolution of the second mode images [14].

In previous works, all focus is on higher contrast and more stiffness sensitivity which is caused by exciting higher modes and no one has investigated how to increase the probability of second mode excitation. In this paper, a rectangular cantilever in air medium has been considered. The cantilever has been modeled by the Timoshenko beam model, and exact models have been employed for the forces of interaction between tip and sample. The orientation angle of cantilever relative to sample, dimensions of the probe and the mass of the tip have not been disregarded. In the simulations, all the geometrical parameters have been changed one by one, the second-to-first mode frequency ratios have been computed and the dimensions that yield the minimum frequency ratio have been chosen as the optimal dimensions.

To validate the results, the sensitivity of the second mode to sample stiffness, which is a measure of AFM sensitivity, was investigated and it was found that by optimizing each of the geometrical parameters, the sensitivity of the second mode and consequently the image contrast can be increased relative to cantilevers with suboptimal dimensions.

Fig. 1 Schematic of an angled AFM cantilever whose tip

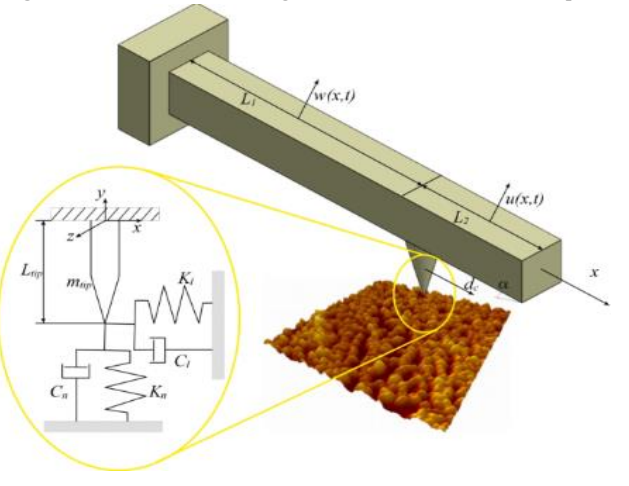

is not located at the end

This paper provides a good guideline for the designers and users of atomic force microscopes so that, in

consideration of a range of sample stiffness values and geometrical parameters, they can choose a cantilever that increases the self-excitation probability of the second mode and thus generates a higher sensitivity.

2 MATHEMATICAL MODELING

All For the purpose of mathematical modeling, a uniformly rectangular cantilever beam with a conical tip un-parallel to sample has been considered (Fig. 1). By the way, the tip is not located at the end of the cantilever.

In the above figure, parameters m_{tip}, α, L_{tip} and d_c respectively represent the tip mass, angle between cantilever and sample, distance between the neutral axis of cantilever and the end of tip and the distance between the lower edge of cantilever and the tip's center of mass.

If axial forces are disregarded, the governing equations of the beam will be written as follows:

$$P.D.Es:$$

$$\frac{\partial}{\partial x}\left[kGA\left(\frac{\partial w(x,t)}{\partial x}-\psi(x,t)\right)\right]-c\frac{\partial w(x,t)}{\partial t}-\rho A\frac{\partial^2 w(x,t)}{\partial t^2}=0 \qquad -L_1 \le x \le 0$$

$$\frac{\partial}{\partial x}\left[EI\left(\frac{\partial \psi(x,t)}{\partial x}\right)\right]+kGA\left(\frac{\partial w(x,t)}{\partial x}-\psi(x,t)\right)-\rho I\frac{\partial^2 \psi(x,t)}{\partial t^2}=0$$

$$P.D.Es:$$

$$\frac{\partial}{\partial x}\left[kGA\left(\frac{\partial u(x,t)}{\partial x}-\phi(x,t)\right)\right]-c\frac{\partial u(x,t)}{\partial t}-\rho A\frac{\partial^2 u(x,t)}{\partial t^2}=0 \qquad 0 \le x \le L_2$$

$$\frac{\partial}{\partial x}\left[EI\left(\frac{\partial \phi(x,t)}{\partial x}\right)\right]+kGA\left(\frac{\partial u(x,t)}{\partial x}-\phi(x,t)\right)-\rho I\frac{\partial^2 \phi(x,t)}{\partial t^2}=0 \qquad (1)$$

Since the tip is not completely positioned at the end of the cantilever, in the above equations, the transverse deformation and the bending angle are designated as u and ϕ, respectively, for the right section of cantilever, and as w and ψ, for the left section of cantilever. The cantilever angled with respect to sample is simulated for a rectangular cross section, and the vertical interaction forces are approximated by two linear spring and damper forces, and the boundary conditions are derived as follows:

$$\begin{aligned} &w(-L_0,t)=0\\ &\psi(-L_0,t)=0\\ &w(0,t)=u(0,t)\\ &\psi(0,t)=\phi(0,t) \end{aligned} \qquad (2)$$

$$\begin{aligned} &EI\left(\frac{\partial \psi(0,t)}{\partial x}-\frac{\partial \phi(0,t)}{\partial x}\right)=\\ &\frac{H}{2}(K_n-K_l)w(0,t)\sin 2\alpha+\\ &\frac{H}{2}(C_n-C_l)\frac{\partial w(0,t)}{\partial t}\sin 2\alpha-\\ &H^2(K_n\sin^2\alpha+K_l\cos^2\alpha)\psi(0,t)\\ &-H^2(C_n\sin^2\alpha+C_l\cos^2\alpha)\frac{\partial \psi(0,t)}{\partial t}\\ &-m_{tip}d_c{}^2\frac{\partial^2 \psi(0,t)}{\partial t^2} \end{aligned} \qquad (3)$$

$$\begin{aligned} &kGA\left(\frac{\partial u(0,t)}{\partial x}-\phi(0,t)\right)-kGA\left(\frac{\partial w(0,t)}{\partial x}-\psi(0,t)\right)=\\ &\frac{H}{2}(K_l-K_n)\psi(0,t)\sin 2\alpha+\frac{H}{2}(C_l-C_n)\frac{\partial \psi(0,t)}{\partial t}\sin 2\alpha+\\ &m_{tip}\frac{\partial^2 w(0,t)}{\partial t^2}+(K_n\cos^2\alpha+K_l\sin^2\alpha)w(0,t)+\\ &(C_n\cos^2\alpha+C_l\sin^2\alpha)\frac{\partial w(0,t)}{\partial t} \end{aligned} \qquad (4)$$

$$\frac{\partial \phi(L_2,t)}{\partial x}=0 \qquad (5)$$

$$\frac{\partial u(L_2,t)}{\partial x}-\phi(L_2,t)=0 \qquad (6)$$

Boundary conditions (2) indicate that displacement and slope are zero at the fixed end of the beam and continuous at the location where the sample is. Boundary conditions (3) and (4) respectively indicate that there are moment equilibrium and force equilibrium at the location where the probe is attached to the cantilever. And finally, Boundary conditions (5) and (6) respectively point out that zero moment and zero force exist at the free end of the cantilever. Using the Finite Element Method, the above equations are written as follows:

$$([M]+[m_{tip}])\{\ddot{d}\}+[C]\{\dot{d}\}+[K]\{d\}=\{F_e\}+\{F_{\text{int}}\} \qquad (7)$$

Where $[M]$, $[C]$ and $[K]$ are the mass matrix, structural damping matrix and the stiffness matrix of the rectangular cantilever by means of the Timoshenko beam model [15].

And $[m_{tip}]$ is the mass matrix of the cantilever tip, which, for the element where the tip is located, is equal to:

$$[m_{tip}]=\begin{bmatrix} m_{tip} & 0\\ 0 & d_c{}^2 m_{tip}\end{bmatrix} \qquad (8)$$

And for the rest of the nodes, it is considered equal to zero. $\{F_e\}$ and $\{F_{\text{int}}\}$ are the matrix of base excitation force and the matrix of interaction force between sample and cantilever tip, respectively; and the interaction force between tip and sample can be represented by an equivalent spring and damping system and expressed as follows:

$$\{F_{\text{int}}\} = [K_{\text{int}}]\begin{Bmatrix} d \\ \theta \end{Bmatrix} + i\omega[C_{\text{int}}]\begin{Bmatrix} \dot{d} \\ \dot{\theta} \end{Bmatrix} \quad (9)$$

Where the stiffness and the damping matrixes of the interaction force for the case in which the cantilever is not parallel to sample will be:

$$K_{\text{int}} = \begin{bmatrix} K_n \cos^2\alpha + K_l \sin^2\alpha & l_{tip}\cos\alpha\sin\alpha(K_l - K_n) \\ l_{tip}\cos\alpha\sin\alpha(K_l - K_n) & l_{tip}{}^2(K_l\cos^2\alpha + K_n\sin^2\alpha) \end{bmatrix} \quad (10)$$

$$C_{\text{int}} = \begin{bmatrix} C_n \cos^2\alpha + C_l \sin^2\alpha & l_{tip}\cos\alpha\sin\alpha(C_l - C_n) \\ l_{tip}\cos\alpha\sin\alpha(C_l - C_n) & l_{tip}{}^2(C_l\cos^2\alpha + C_n\sin^2\alpha) \end{bmatrix} \quad (11)$$

K_n, K_l, C_n and C_l denote the vertical contact stiffness, tangential contact stiffness, vertical contact damping and tangential contact damping between cantilever tip and sample, respectively. Considering the air medium and using the Van der Waals and the DMT model for the attractive region and repulsive region of the vertical forces respectively and applying the Hertz force model for the tangential force, these coefficients will be as follows [16], [17]:

$$K_n = -\frac{\partial F_n}{\partial d}\Big|_{d=D_0} = \begin{cases} -\dfrac{HR_t}{3D_0{}^3} & d \ge a_0 \\ 2E_{eff}\sqrt{R_t}(a_0 - D_0)^{\frac{1}{2}} & d < a_0 \end{cases} \quad (12)$$

$$K_l = -\frac{\partial F_l}{\partial d}\Big|_{d=D_0} = \begin{cases} 0 & d \ge a_0 \\ 8G_{eff}\left(\dfrac{3R_t f_c}{4E_{eff}}\right)^{\frac{1}{3}} & d < a_0 \end{cases} \quad (13)$$

$$C_n = -\frac{\partial F_n}{\partial \dot{d}}\Big|_{d=D_0} = \begin{cases} 0 & d \ge a_0 \\ \eta_n(a_0 - D_0)^{\frac{1}{2}} & d < a_0 \end{cases} \quad (14)$$

$$C_l = -\frac{\partial F_n}{\partial \dot{d}}\Big|_{d=D_0} = \begin{cases} 0 & d \ge a_0 \\ \eta_l & d < a_0 \end{cases} \quad (15)$$

In the above equations, H is the Hamaker constant, R_t is the cantilever tip radius, d is the vertical distance between cantilever tip and sample surface, a_0 is the intermolecular distance, E_{eff} is the effective elasticity modulus between sample and cantilever tip, G_{eff} is the effective shear modulus between sample and cantilever tip, η_n is the contact viscosity between tip and sample in the vertical direction and η_l is the contact viscosity between tip and sample in the tangential direction. By inserting the interaction force into Eq. 7, the frequency response of the system will be expressed as:

$$\frac{\{\phi\}}{A} = \frac{(\omega^2([M]+[m_{tip}]) - i\omega[C_{\text{int}}] - [K_{\text{int}}])\{1,0,1,0,...\}^T}{(-\omega^2([M]+[m_{tip}]) + i\omega[C+C_{\text{int}}] + [K+K_{\text{int}}])} \quad (16)$$

Table 1 The Parameter related silicon cantilever[2].

Cantilever and tip parameters	Magnitude
Cantilever length(L)	$252\mu m$
Cantilever width(b)	$35\mu m$
Cantilever thickness(h)	$2.3\mu m$
Angle between cantilever and sample (α)	$30\deg$
Tip length(l_{tip})	$10\mu m$
Tip Radius(R_{tip})	$10nm$
Tip Mass(m_e)	$0.06\rho bhL$
Cantilever mass density(ρ)	$2330(kg/m^3)$
Cantilever elasticity modulus(E)	$130GPa$
Damping of tip-sample in normal direction (C_n)	$1x10^{-2}N\ s/m^2$
Damping of tip-sample in tangential direction (C_l))	$1x10^{-3}N\ s/m^2$
Intermolecular distance (a_0)	$0.38nm$
Hamaker constant in air (H_{air})	$2.96x10^{-19}J$

In the above equation, A is the amplitude of the base excitation force. By plotting the frequency response, the frequency, amplitude and the phase of the first n modes can be obtained. Since by changing the geometrical parameters, the mass matrix, cantilever stiffness and the stiffness and damping of interaction also change, it is predictable to have different frequency ratios with the change of geometrical parameters.

3 SIMULATIONS AND RESULTS

In this paper, the optimal geometrical parameters of a rectangular cantilever in air medium that produce the highest frequency sensitivity in the second mode have been obtained and the diagrams of frequency sensitivity vs. sample stiffness for these optimum parameters have been compared with each other.

First, the parameters of the rectangular silicon cantilever and the sample made of HOPG material, with the specifications listed in Table 1, have been investigated as the main values, and the free vibration frequencies of the above cantilever for the first four modes in air have been obtained, which are equal to 43.7, 273.7, 767.7 and 1501.9 kHz, respectively. In Table 2, the frequency ratios of modes obtained from simulations have been compared with the theoretical values [12], and a good agreement between them has been observed.

Table 2 Comparison between simulation and theoretical frequency ratios [12]

Frequency ratio / Methods	$\frac{\omega_2}{\omega_1}$	$\frac{\omega_3}{\omega_1}$	$\frac{\omega_4}{\omega_1}$
Simulation	6.263	17.567	34.37
Theoretical	6.27	17.55	34.39

Then, by considering the interaction forces and changing the geometrical parameters of cantilever and tip, the frequency ratios have been computed. In the graphs of Fig. 2, the second-to-first mode frequency ratios vs. the variation of geometrical parameters listed in Table 3 have been illustrated. In each section, by changing one parameter and keeping the other parameters constant according to Table 1, the second-to-first mode frequency ratio has been plotted. In view of these graphs, the optimum value of each parameter that minimizes the corresponding frequency ratio can be obtained. The second-to-first mode frequency ratio of a cantilever with a uniform and homogeneous rectangular cross section is 6.27 [12]. Nevertheless, by considering the effect of interaction forces and changing the geometrical parameters, this value can be adequately reduced to increase the self-excitation probability of the second mode relative to first mode.

In Fig. 2(a), by changing the cantilever length from 150 to 300 μm, the changes of frequency ratio with cantilever length have been illustrated. As it is observed, the minimum frequency ratio (2.36) occurs at the length of 195 μm. In Fig. 2(b), frequency ratio has been plotted by changing the cantilever thickness from 1.15 to 3.45 μm and keeping the other parameters constant. The minimum frequency ratio (2.38) occurs at the cantilever thickness of 3.05 μm. In Fig. 2(c), frequency ratio has been plotted by changing the cantilever width from 20 to 50 μm. As it is shown in this section, by increasing the cantilever width, the frequency ratio diminishes; however, since the maximum width in this range is 50 μm, this is considered as the optimum width, and the minimum frequency ratio at this width is 2.42.

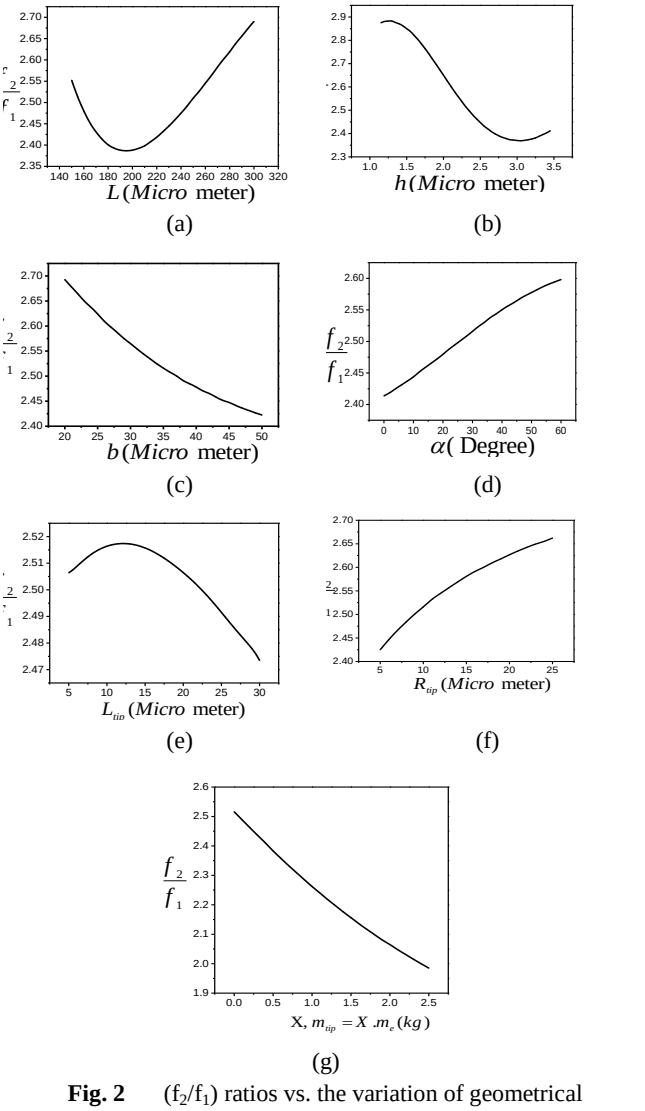

Fig. 2 (f_2/f_1) ratios vs. the variation of geometrical parameters; (a) Cantilever length, (b) Cantilever thickness, (c) Cantilever width, (d) Angle between cantilever and sample surface, (e) Tip length, (f) Tip radius, (g) Tip mass

Fig. 2(d) demonstrates that the frequency ratio increases with the increase of the angle between cantilever and sample surface. Thus, the minimum frequency ratio of 2.41 is obtained at the optimum orientation angle of zero. The effect of probe length on frequency ratio has been sketched in Fig. 2(e). The length of probe varies from 5 to 30 μm, and as the probe length increases beyond 12 μm, the frequency

ratio starts to diminish. Therefore, the minimum frequency ratio occurs at the end of the tip length range (30 μm) and its value at that length is 2.47. In Fig. 2(f), the changes of frequency ratio with tip radius (varying between 5 and 25 nm) have been plotted.

As this graph indicates, the smaller the tip radius is, the lower the frequency ratio will be; so in the beginning of this radius interval (tip radius of 5 nm), the minimum frequency ratio (2.425) is obtained. Also, in the repulsive range, as the tip radius becomes smaller, a more stable solution is achieved; and with the increase of tip radius, the repulsive force becomes stronger and the tip cannot contact the sample more often and the solution quickly becomes unstable. Finally, In Fig. 2(g), by varying the tip mass between 0 and 2.5 times, the chosen mass or m_e, the second-to-first mode frequency ratio has been plotted. As this graph shows, the frequency ratio diminishes with the increase of tip mass; and the minimum frequency ratio of 1.985 is obtained for a tip mass which is 2.5 times the chosen mass.

Now by calculating the optimal values obtained from the graphs of Fig. 2, the frequency sensitivities of the second vibration mode with respect to the changes of elasticity and sample stiffness have been plotted in Fig. 3 graphs.

Since the second mode will become sensitive in the elasticity range of more than 10 GPa, the range of elasticity changes has been illustrated for three distinct intervals between 10 to 100 GPa and designated by Sections (a), (b) and (c). As it is observed, by considering the optimal cantilever length of 195 μm, the highest frequency sensitivity of the second mode is achieved in the entire elasticity interval; therefore, by changing the cantilever length, provided that it produces the minimum frequency ratio, the highest contrast can be achieved at the excitation of higher modes.

After length, the highest sensitivity in the elasticity interval of 10-28.7 GPa belongs to the optimal tip mass, and after that, up to an elasticity of 65 GPa, the highest sensitivity belongs to the optimal cantilever thickness (i.e., 3.05 μm). However, for hard materials, with elasticity values between 65 and 100 GPa, the frequency sensitivity of the second mode will be higher for the optimal probe length than for cantilever thickness; while for soft materials in Fig. 3(a), the frequency sensitivity for the optimal probe length is even less than the sensitivity of a cantilever with the suboptimal dimensions specified in Table 1. This indicates that, for hard materials with a high elasticity, maximum contrast can be achieved by changing the probe length that leads to the minimization of the second-to-first mode frequency ratio; but of course, this contrast will be lower in quality than that achieved for optimum length. Also, as the graphs illustrate, for materials with elasticity values between 20 and 100 GPa, by optimizing each of the geometrical parameters, the sensitivity of the second mode and consequently the achieved contrast can be increased relative to cantilevers with suboptimal dimensions.

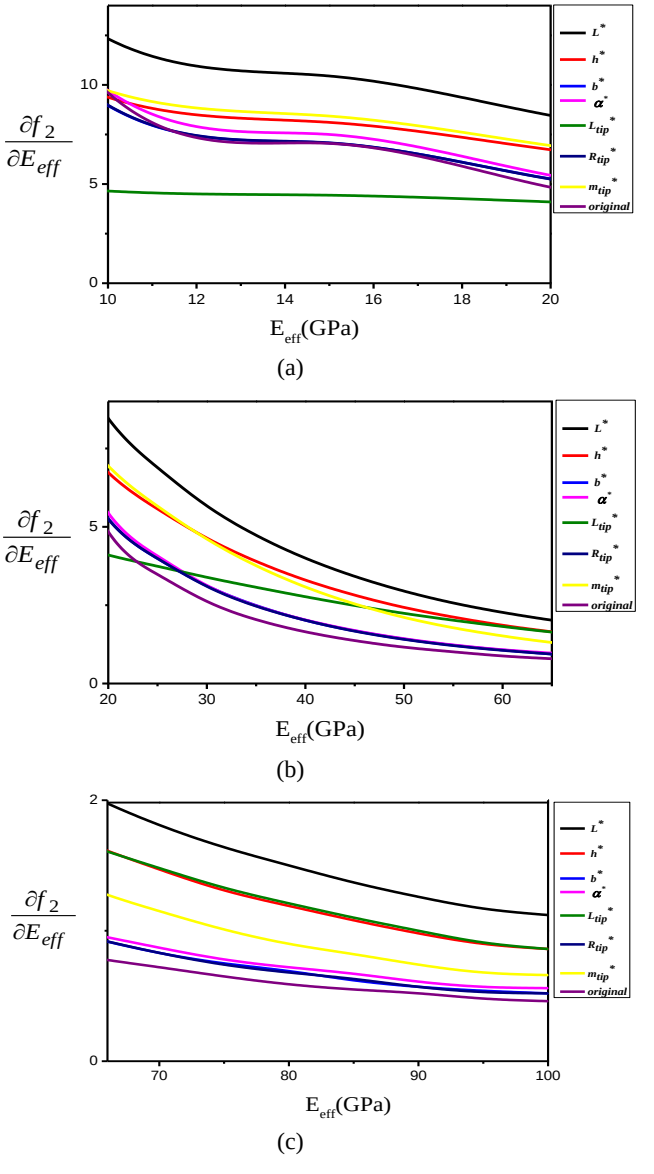

Fig. 3 Sensitivity of second mode to sample stiffness for optimum parameters that yield the minimum frequency ratio; (a) Elasticity interval of 10 to 20 GPa, (b) Elasticity interval of 20 to 65 GPa, (c) Elasticity interval of 65 to 100 GPa

Moreover, regarding the orientation angle of cantilever, it can be seen that, in the whole range of elasticity, the sensitivity of the second mode is higher for the optimal orientation angle than for the optimal width of cantilever; however, this discrepancy is more pronounced for soft materials in Fig. 3(a) and for very hard materials in Fig. 3(c).

In this section, to clarify the theoretical results, the empirical results obtained from topography in the first and second modes of a cantilever which only has an optimal length or produces the minimum frequency ratio have been compared in Fig. 4. The images clearly show that the contrast is much higher for the cantilever with optimum dimensions and that it can better discern between different materials. This shows the importance of using a cantilever that produces the minimum frequency ratio; because in this case, the sensitivity of the second mode to the change of material type increases and the properties of different materials are distinguished more clearly. In addition, with the frequency ratio becoming small, the self-excitation probability of the second mode due to the excitation of the first mode increases, and consequently, a better contrast can be achieved.

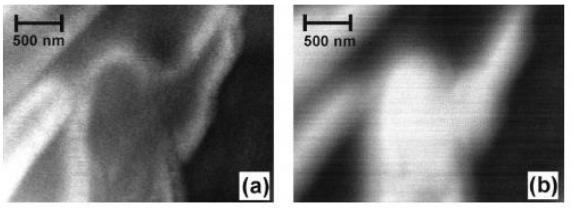

Fig. 4 Topography of C60 on HOPG [14]; (a) First mode excitation, (b) Second mode excitation [14]

Although in this paper, cantilever dimensions have been optimized with the intension of second mode excitation and increasing the sensitivity of the second mode, to more thoroughly investigate the subject of sensitivity, the frequency sensitivity of the first mode to sample stiffness has been computed for all the optimal parameters and compared with the those of cantilevers with suboptimal dimensions in the graphs plotted in Fig. 5.

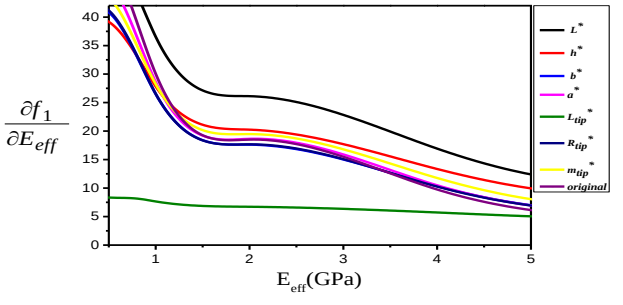

Fig. 5 Sensitivity of the first mode to sample stiffness for optimum parameters that produce the minimum frequency ratio

Interestingly, in the entire first mode sensitivity range (0.001-5 GPa), the sensitivity of the first mode is the highest for the cantilever with optimal length that produces the minimum frequency ratio. After that, in the elasticity range of 1.1-5 GPa, the cantilever with optimal thickness produces the highest frequency sensitivity in the first mode, followed by the cantilever with optimum tip mass. However, regarding the rest of the parameters, e.g. the orientation angle of cantilever with respect to sample, the sensitivity of the first mode relative to the normal mode does not show a noticeable change; and for a cantilever with optimal width, tip radius and probe length, the sensitivity of the first mode relative to the normal mode gets even worse, with the probe length causing the most considerable worsening.

4 CONCLUSION

In this paper, geometrical parameters have been proposed for rectangular cantilevers that can increase the contrast and sensitivity of the atomic force microscope at second mode excitation. The excitation of this mode occurs as separate excitation, simultaneous excitation with the first mode in bimodal microscopes or as self-excitation due to excitation of first mode. Since by exciting the second mode, additional information on sample properties can be acquired and thus the resolution of AFM images can be improved, the designing of a cantilever that has the highest sensitivity at the second mode is important; and using such a cantilever, more accurate results can be obtained.

The results indicate that by changing the geometrical parameters, provided that it produces the minimum second-to-first mode frequency ratio, the self-excitation probability of the second mode can be increased and also a higher frequency sensitivity at the second mode can be achieved. Moreover, of the geometrical parameters considered in the simulation results, cantilever length has the greatest effect on improving the resolution and contrast of images; and by selecting a length that generates the minimum frequency ratio, the highest frequency sensitivity can be obtained at the second, and even first mode.

Following the cantilever length, the highest sensitivity for soft materials can be achieved by optimizing the tip mass; and for materials with elasticity values between 28 and 65 GPa, the minimum frequency ratio can be obtained by optimizing the cantilever length. For very hard materials, the highest sensitivity, after the sensitivity of the optimal cantilever length, belongs to the optimal tip length. It should be mentioned that, for hard samples, the effect of probe length is very important; and by making the probe longer, a higher sensitivity at the second mode can be obtained for these kinds of samples. On the contrary, for soft samples, images with a higher resolution can be obtained through the excitation of the second mode, by decreasing the orientation angle of cantilever relative to sample.

ACKNOWLEDGMENTS

The author would like to express her gratitude to the Islamic Azad University, Shahr-e-Qods Branch, Tehran, Iran. paper is extracted from the research project with title of " Improvement of Multifrequency AFM response (Bimodal and Trimodal) in air and liquid environment in comparison to single mode AFM".

REFERENCES

[1] Martin, Y., C. Williams, and H. K., Wickramasinghe, "Atomic Force Microscope–Force Mapping and Profiling on a Sub 100-Å Scale", Journal of Applied Physics, Vol. 61, No. 10, 1987, pp. 4723-4729.

[2] Stark, M., et al., "From Images to Interactions: High-Resolution Phase Imaging in Tapping-Mode Atomic Force Microscopy", Biophysical journal, Vol. 80, No. 6, 2001, pp. 3009-3018.

[3] Xu, X., et al., "Unmasking Imaging Forces on Soft Biological Samples in Liquids when using Dynamic Atomic Force Microscopy, A Case Study on Viral Capsids", Biophysical journal, Vol. 95, No. 5, 2008, pp. 2520-2528.

[4] Stark, M., et al., "Inverting Dynamic Force Microscopy: From Signals to Time-Resolved Interaction Forces", Proceedings of the National Academy of Sciences, Vol. 99, No. 13, 2002, pp. 8473-8478.

[5] Legleiter, J., et al., "Scanning Probe Acceleration Microscopy (SPAM) in Fluids: Mapping Mechanical Properties of Surfaces at the Nanoscale", Proceedings of the National Academy of Sciences of the United States of America, Vol. 103, No. 13, 2006, pp. 4813-4818.

[6] Hillenbrand, R., M. Stark, and R. Guckenberger, "Higher-Harmonics Generation in Tapping-Mode Atomic-Force Microscopy: Insights into the Tip–Sample Interaction", Applied Physics Letters, Vol. 76, No. 23, 2000, pp. 3478-3480.

[7] Sahin, O., A. Atalar, "Simulation of Higher Harmonics Generation in Tapping-Mode Atomic Force Microscopy", Applied Physics Letters, Vol. 79, No. 26, 2001, pp. 4455-4457.

[8] Stark, R.W., "Spectroscopy of Higher Harmonics in Dynamic Atomic Force Microscopy", Nanotechnology, Vol. 15, No. 3, 2004, pp. 347.

[9] Sharos, L., et al., "Enhanced Mass Sensing using Torsional and Lateral Resonances in Microcantilevers", Applied Physics Letters, Vol. 84, No. 23, 2004, pp. 4638-4640.

[10] Basak, S., A. Raman, "Dynamics of Tapping Mode Atomic Force Microscopy in Liquids: Theory and Experiments", Applied Physics Letters, Vol. 91, No. 6, 2007, pp. 064107.

[11] Melcher, J., et al., "Origins of Phase Contrast in the Atomic Force Microscope in Liquids", Proceedings of the National Academy of Sciences, Vol. 106, No. 33, 2009, pp.13655-13660.

[12] Garcia, R., E. T. Herruzo, "The Emergence of Multifrequency Forces Microscopy", Nature nanotechnology, Vol. 7, No. 4, 2012, pp. 217-226.

[13] Rodrıguez, T. R., R. García, "Compositional Mapping of Surfaces in Atomic Force Microscopy by Excitation of the Second Normal Mode of the Microcantilever", Applied Physics Letters, Vol. 84, No. 3, 2004, pp. 449-451.

[14] Sadewasser, S., Villanueva, G. and Plaza, J. "Special Cantilever Geometry for the Access of Higher Oscillation Modes in Atomic Force Microscopy", Applied physics letters, Vol. 89, No. 3, 2006, pp. 033106.

[15] Damircheli, M., M. Korayem, "Dynamic Analysis of the AFM by Applying the Timoshenko Beam Theory in the Tapping Mode and Considering the Impact of the Interaction Forces in a Liquid Environment", Canadian Journal of Physics, Vol. 92, No. 6, 2013, pp. 472-483.

[16] Johnson, K., "Contact Mechanics", Cambridge University Press, Cambridge, 1985, UK.

[17] Derjaguin, B., V. Muller, and Y. P. Toporov, "Effect of Contact Deformations on the Adhesion of Particles", Journal of Colloid and interface science, Vol. 53, No. 2, 1975, pp. 314-326.

[18] Song, Y., B. Bhushan, "Finite-Element Vibration Analysis of Tapping-Mode Atomic Force Microscopy in Liquid", Ultramicroscopy, Vol. 107, No. 2, 2007, pp. 1095-1104.